GE Energy

James C. Kinsey
Project Manager, ESBWR Licensing

PO Box 780 M/C J-70
Wilmington, NC 28402-0780
USA

T 910 675 5057
F 910 362 5057
jim.kinsey@ge.com

MFN 06-135
Supplement 2

Docket No. 52-010

January 23, 2007

U.S. Nuclear Regulatory Commission
Document Control Desk
Washington, D.C. 20555-0001

Subject: **Response to Portion of RAI Letter Number 20 Related to ESBWR Design Certification Application – Seismic Design – RAI Numbers 3.7-6S01 and 3.7-48S02**

Enclosure 1 contains supplemental responses to the subject RAIs resulting from the November 2006 NRC Seismic Audit. GE's prior responses were transmitted via the Reference 1 and Reference 2 letters. There are no changes to any of the remaining RAI responses contained in the Referenced letters.

If you have any questions or require additional information regarding the information provided here, please contact me.

Sincerely,

Kathy Sedney for

James C. Kinsey
Project Manager, ESBWR Licensing

D068

Enclosure:

1. MFN 06-135, Supplement 2 - Response to Portion of RAI Letter Number 20 Related to ESBWR Design Certification Application – Seismic Design – RAI Numbers 3.7-6S01 and 3.7-48S02

References:

1. MFN 06-135, Letter from David H. Hinds to U. S. Nuclear Regulatory Commission, *Partial Response to RAI Letter Numbers 20 and 27 Related to ESBWR Design Certification Application – Seismic Design – DCD Sections 2.5 and 3.7 – RAI Numbers 2.5-2 through 2.5-7; 3.7-1 through 3.7-4, 3.7-6, 3.7-9, 3.7-10, 3.7-13 through 3.7-15, 3.7-17 through 3.7-23, 3.7-28, 3.7-31, 3.7-36, 3.7-40 through 3.7-49, 3.7-51, 3.7-53, and 3.7-56,* May 23, 2006
2. MFN 06-135, Supplement 1, Letter from David H. Hinds to U. S. Nuclear Regulatory Commission, *Response to Portion of RAI Letter Number 20 Related to ESBWR Design Certification Application – Seismic Design – RAI Numbers 3.7-2, 3.7-13, 3.7-17, 3.7-18, 3.7-19, 3.7-21, 3.7-22, 3.7-36, 3.7-40, 3.7-47, 3.7-48, 3.7-49, 3.7-51, and 3.7-53 – SUPPLEMENT 1,* October 17, 2006

cc: AE Cubbage USNRC (with enclosures)
GB Stramback GE/San Jose (with enclosures)
eDRF 0000-0060-8442

ENCLOSURE 1

MFN 06-135

SUPPLEMENT 2

Response to Portion of RAI Letter Number 20

Related to ESBWR Design Certification Application

Seismic Design

RAI Numbers 3.7-6S01 and 3.7-48S02

Prior Responses previously submitted under MFNs 06-135 and 06-135, Supplement 1 are included to provide historical continuity during review.

NRC RAI 3.7-6

In DCD Section 3.7.1, the applicant stated that seismic design parameters considered for the ESBWR comprise two site conditions: generic sites and ESP sites. In DCD Section 3.7.1.1 and Appendix 3A, the applicant provided a description of two sets of site conditions that are considered in the ESBWR design. In order to assist the staff in performing its review of seismic analyses and design of the reactor building (RB)/fuel building (FB) and control building (CB), the applicant should include a detailed description of the analysis procedures to show (1) how these two sets of seismic design parameters will be applied to perform seismic analyses; (2) how the structural models are combined as a seismic system model; (3) how the seismic analyses (including the soil-structure interaction (SSI) analyses) are performed; and (4) how the analysis results (seismic member forces, sliding forces, overturning moment and floor response spectra) from these two sets of design parameters are to be combined and used for the design. The applicant is requested to provide the above information in the DCD.

GE Response

(1) The two sets of seismic design parameters (generic and North Anna ESP site-specific) are applied separately in performing seismic analyses as described in DCD Sections 3A.3 and 3A.4.1.

(2) The structural models are coupled with the foundation media in the form of soil springs and dampers to form the seismic system model as described in DCD Section 3A.5 and shown in Figures 3A.7-4 and 3A.7-5 for RB/FB and CB, respectively.

(3) The seismic analyses of the seismic system model described above are performed for soil-structure interaction response, using the time history method of analysis described in DCD Section 3A.5.

(4) The analysis results (seismic member forces, sliding forces, overturning moment and floor response spectra) from these two sets of design parameters are enveloped (i.e., worst results among all cases analyzed) and used for the design as described in DCD Section 3A.9.

No DCD change was required in response to this RAI.

NRC RAI 3.7-6, Supplement 1

NRC Assessment Following the November 2, 2006 Audit

Provide justification for the difference in peak amplitudes of the floor response spectra between the single envelope input spectra and the separate RG 1.60 and North Anna spectra.

GE Response

Figure 3.7-6 (1) shows the floor response spectra associated with this comment. There are differences in spectral peaks at about 3 Hz and 11 Hz.

(1) Peak around 11 Hz for the medium site FRS for the RBFB:

The soil conditions for the input motions are different. As shown on Table 3.7-6 (1) the soil conditions (uniform site) are as follows:

For North Anna input motion:	Soil conditions are BE, UB, and LB
For Single Envelope input motion:	Soil conditions are Soft, Medium, Hard, and Fixed

Furthermore, the target spectrum above 10 Hz for the Single Envelope input motion is different from that of the North Anna input motion as shown in Figure 3.7-6 (2).

(2) Peak around 3 Hz for the medium site FRS for the RBFB:

a) Comparison of response spectra

Figure 3.7-6 (2) shows that the target spectra of the two (RG 1.60 and Single Envelope) input motions are identical around 3Hz.

Figure 3.7-6 (3) shows the comparison of two response spectra of input motion used for X-direction with acceleration in normal scale. Figure 3.7-6 (4) shows the ratio of the two response spectra for each frequency. The ratio varies from 0.7 to 1.2

Figures 3.7-6 (5) and 3.7-6 (6) show the comparison and ratio of input motions used for Y-direction. The ratio varies from 0.9 to 1.3.

b) Comparison of FRS at RBFB

Figure 3.7-6 (7) shows the comparison of FRS at RBFB for medium site and X-direction. Figure 3.7-6 (8) shows the ratio of FRS for the two input motions. The ratio varies from 0.7 to 1.8. Around 3 Hz, the ratio is almost 1.5 times of the ratio in Figure 3.7-6 (4).

Figures 3.7-6 (9) and 3.7-6 (10) show the comparison and ratio of FRS for Y-direction. The ratio varies from 0.9 to 1.3. These ratios are almost equal to the ratio in Figure 3.7-6 (6).

Figures 3.7-6 (11) and 3.7-6 (12) show the comparison and ratio of FRS for soft site and X-direction. The ratio varies from 0.8 to 1.5. These ratios show small difference around 1.5Hz compared to Figure 3.7-6 (4).

c) Investigation of FRS using single degree freedom system

For simplicity, a single degree of freedom system is used as a building model as shown in Figure 3.7-6 (13). The natural frequency of single degree of freedom system is determined by the lowest frequency of RBFB considering soil spring for X and Y direction as follows.

X-direction: 3Hz Y-Direction: 2.5Hz

The damping factor of the system is set as h = 0.05.

Figure 3.7-6 (14) shows the comparison of FRS for a single degree of freedom system for X-direction. Figure 3.7-6 (15) shows the ratio of FRS for two input motions. The ratio is almost equal to the ratio in Figure 3.7-6 (8) for RBFB in X-direction.

Figures 3.7-6 (16) and (17) show the results for Y-direction. The ratio is almost equal to the ratio in Figure 3.7-6 (10) for RBFB in Y direction.

Based on these figures, it is determined that the differences of spectral peaks around 3 Hz in the medium site FRS for the RBFB between RG 1.60 input motion and Single Envelope input motion is caused by some difference in the characteristics of input motion and not caused by the analytical model of RBFB.

d) Examination of Fourier spectra for input motion

To examine the characteristics of the two input motions, the Fourier spectrum is calculated. Figure 3.7-6 (18) shows the Fourier spectra of RG 1.60 input motion. Figure 3.7-6 (19) shows the Fourier spectra of Single Envelope input motion.

From the comparison of these two figures, it can be seen that the Fourier amplitude of RG 1.60 input motion is almost three times larger than that of Single Envelope input motion around 3 Hz. The larger Fourier spectrum means larger energy input. Therefore, it is concluded that the difference in Fourier spectra might cause the differences in the spectral peaks around 3 Hz between these two input motions.

(3) Conclusion:

The above discussion explains the differences in spectral peaks around 3 Hz and 11 Hz for the medium site FRS for the RBFB between RG 1.60 input motion, North Anna input motion and Single Envelope input motion. The final design is based on the envelope of all soil cases analyzed.

No DCD change is required in response to this RAI Supplement.

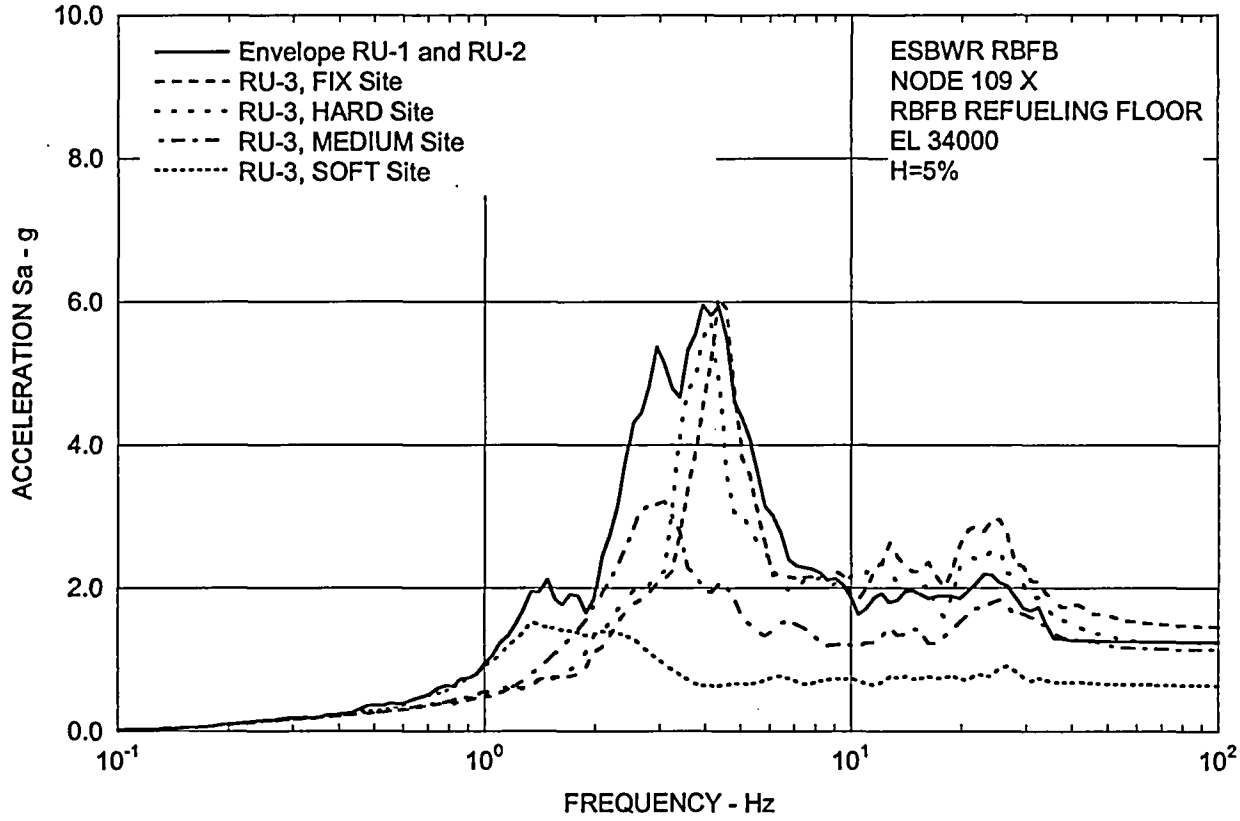

Figure 3.7-6 (1) FRS (Effect of Single Envelope Ground Motion) – RBFB Refueling Floor X

Table 3.7-6 (1) Analysis Cases for Uniform Site

No.	Model	Input Motion	Uniform Soil Condition						
			Generic Site				North Anna ESP Site		
			Soft	Medium	Hard	Fixed	NA-BE	NA-UB	NA-LB
RU-1	Base	RG 1.60 (0.3g)	*	*	*	*			
RU-2	Base	NA site spectra					*	*	*
RU-3	Base	Single envelope spectra	*	*	*	*			

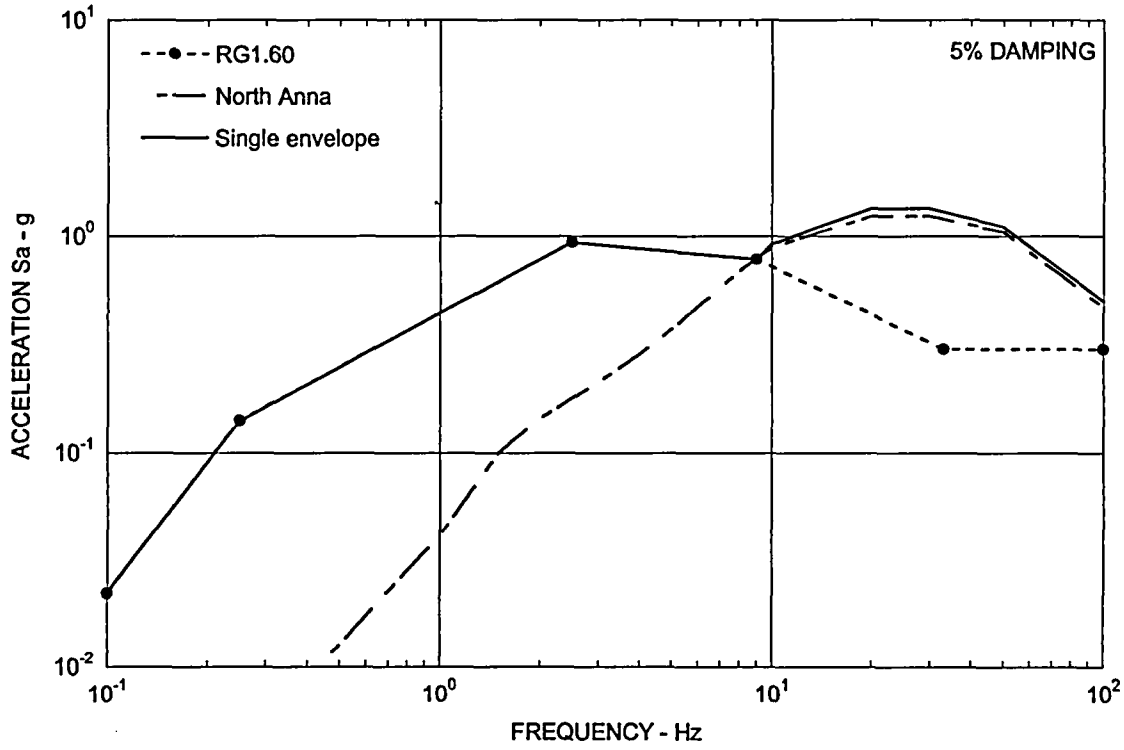

Figure 3.7-6 (2) Comparison of Target Spectra for Horizontal Input Motion

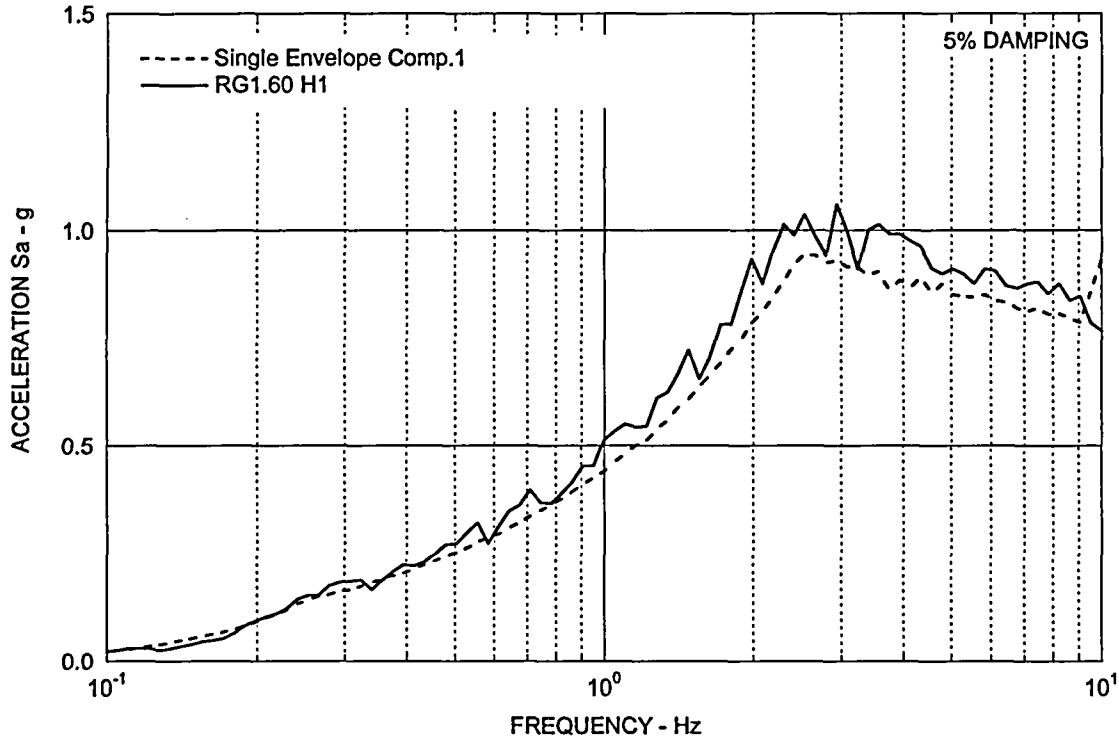

Figure 3.7-6 (3) Response Spectra of Input Motion (H1:for X-Direction)

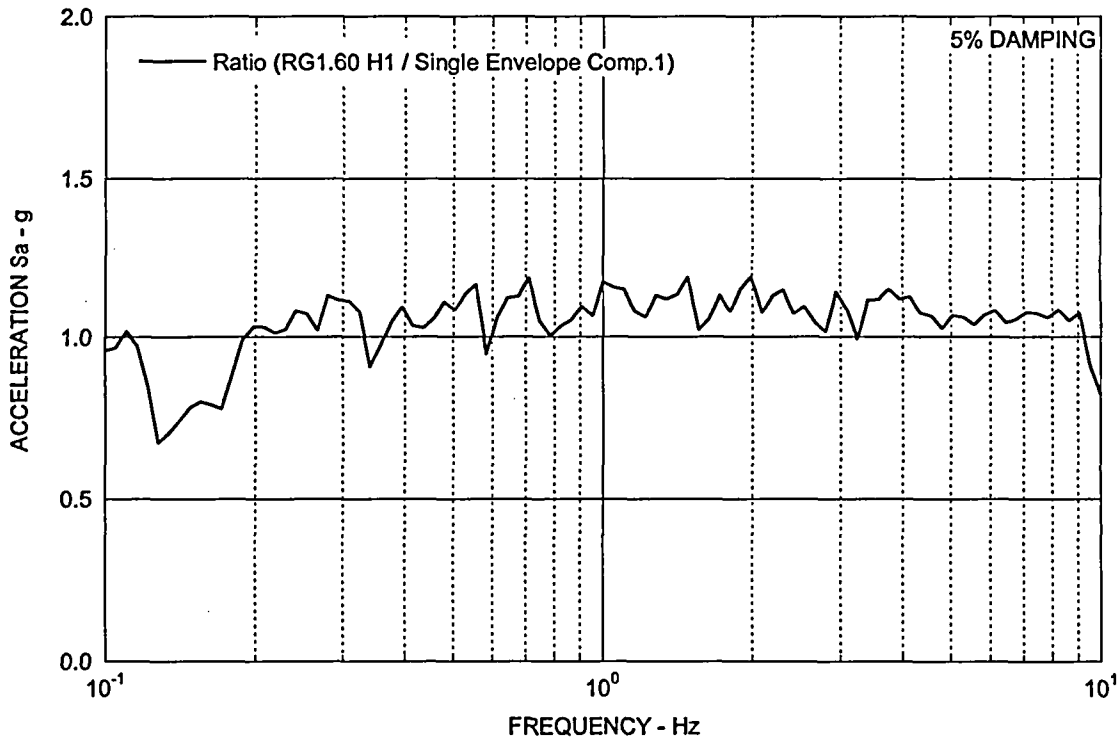

Figure 3.7-6 (4) Ratio of two Response Spectra (H1: for X-Direction)

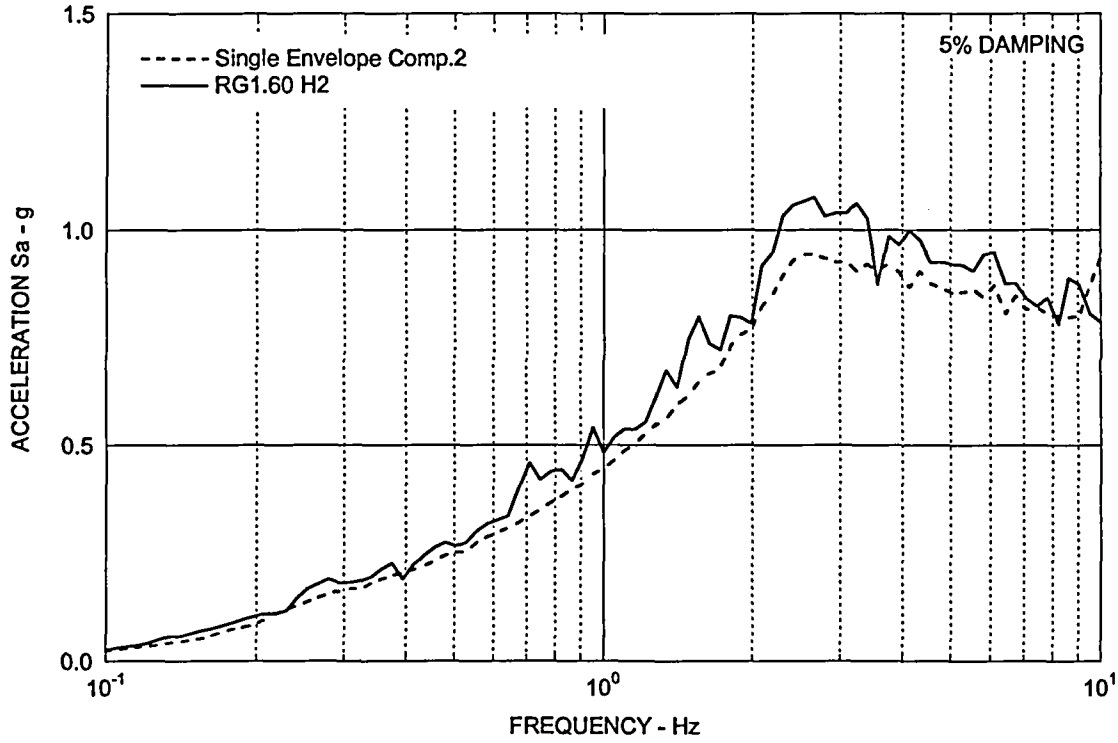

Figure 3.7-6 (5) Response Spectra of Input Motion (H2: for Y-Direction)

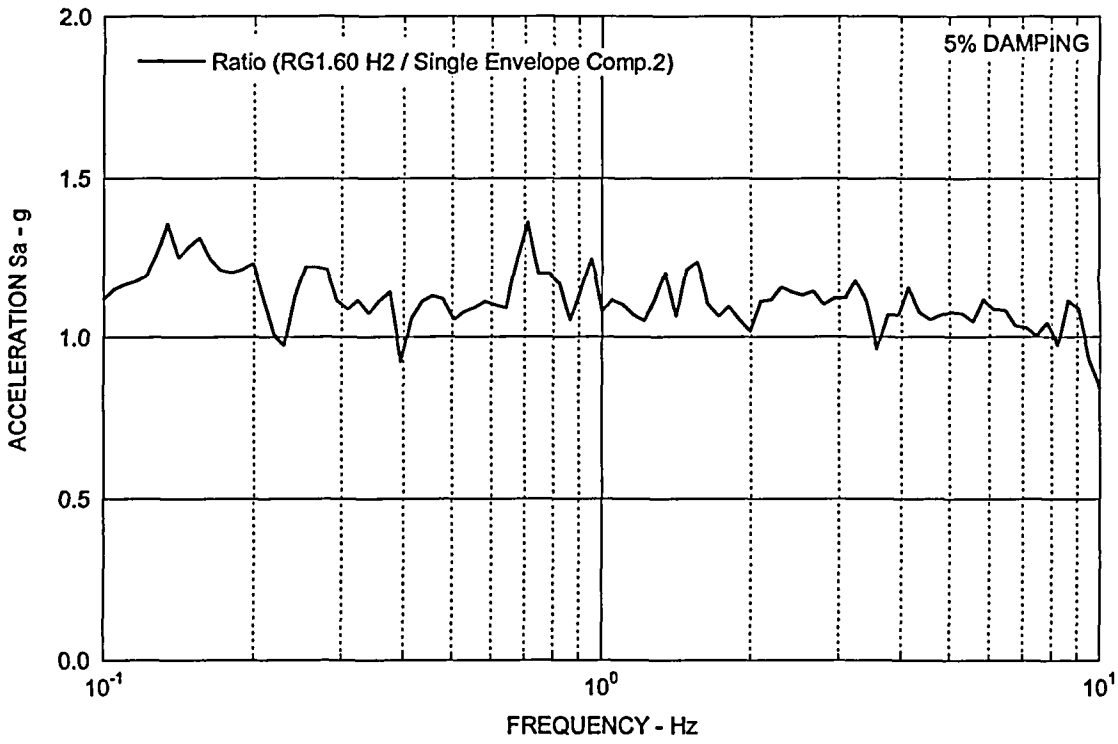

Figure 3.7-6 (6) Ratio of Response Spectra (H2: for Y-Direction)

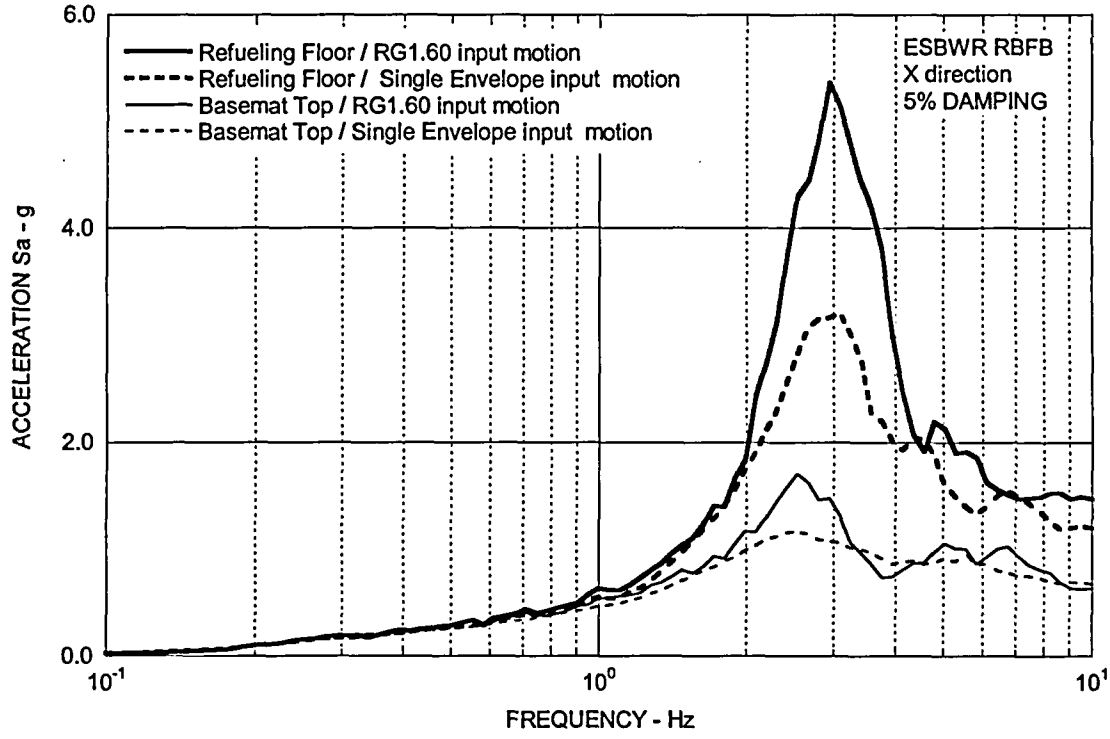

Figure 3.7-6 (7) FRS of RBFB (Medium site: X-Direction)

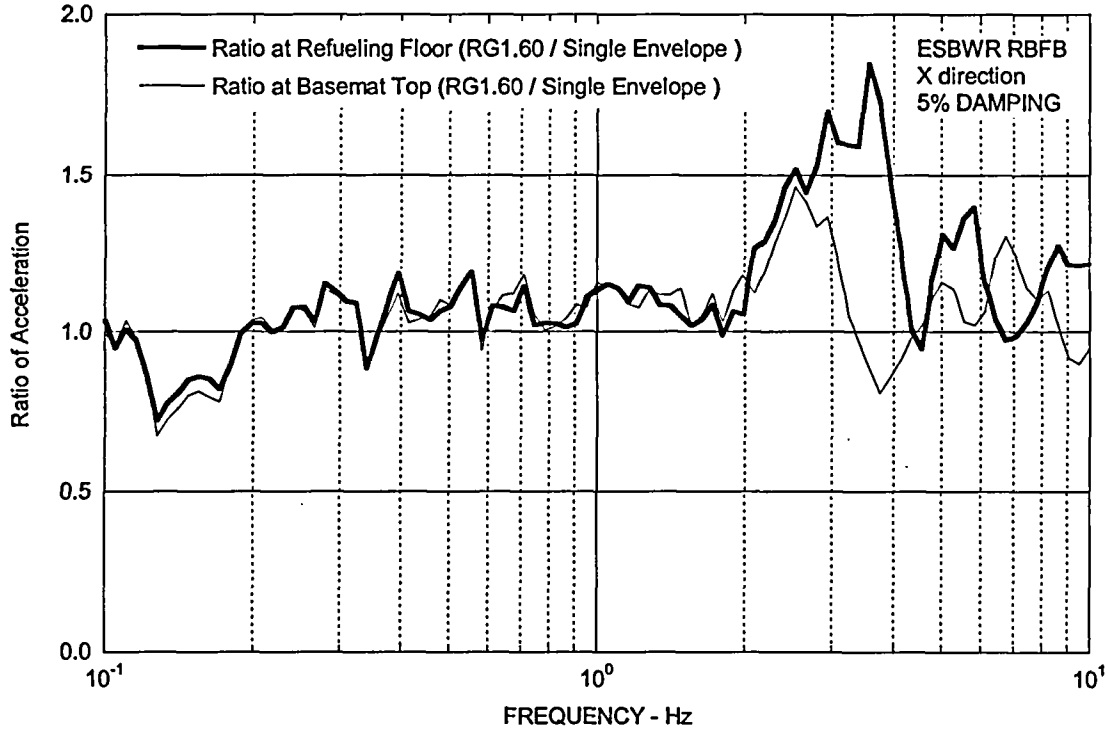

Figure 3.7-6 (8) Ratio of FRS (Medium site: X-Direction)

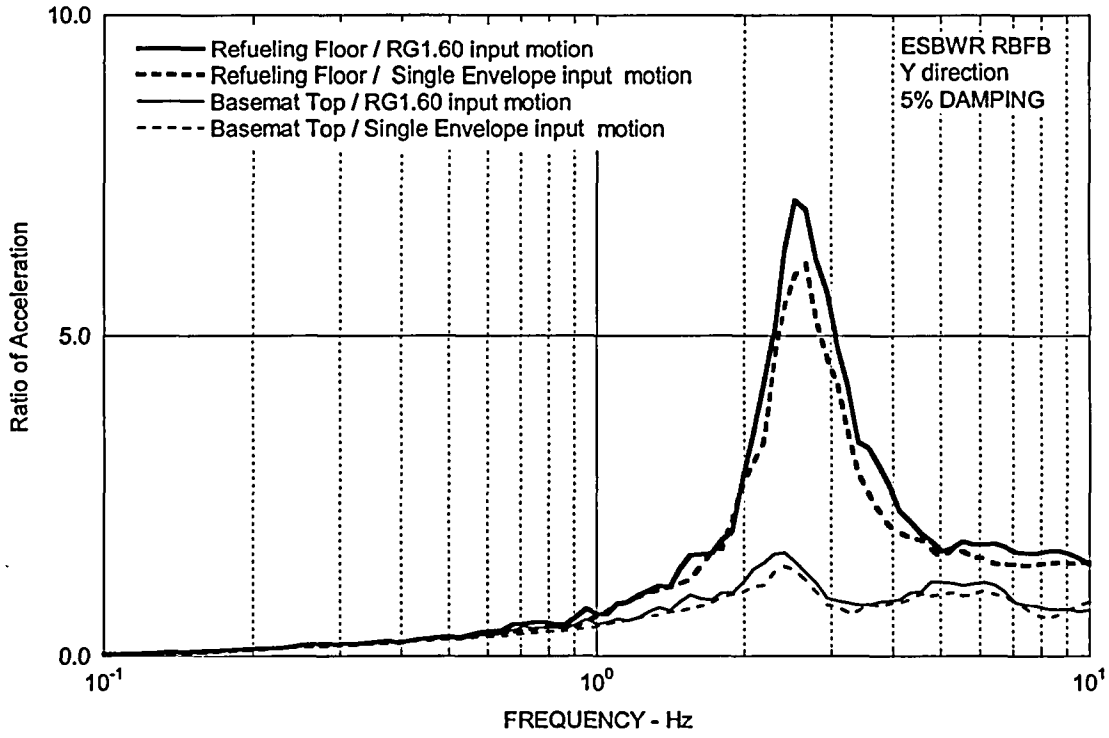

Figure 3.7-6 (9) FRS of RBFB (Medium site: Y-Direction)

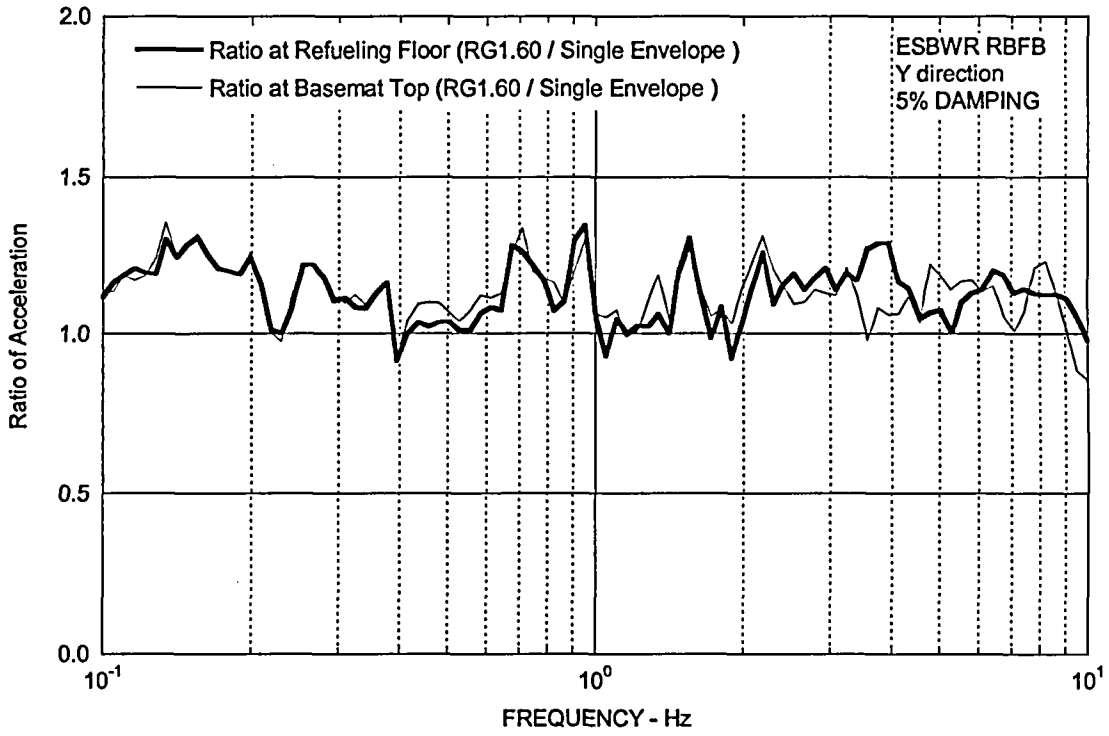

Figure 3.7-6 (10) Ratio of FRS (Medium site: Y-Direction)

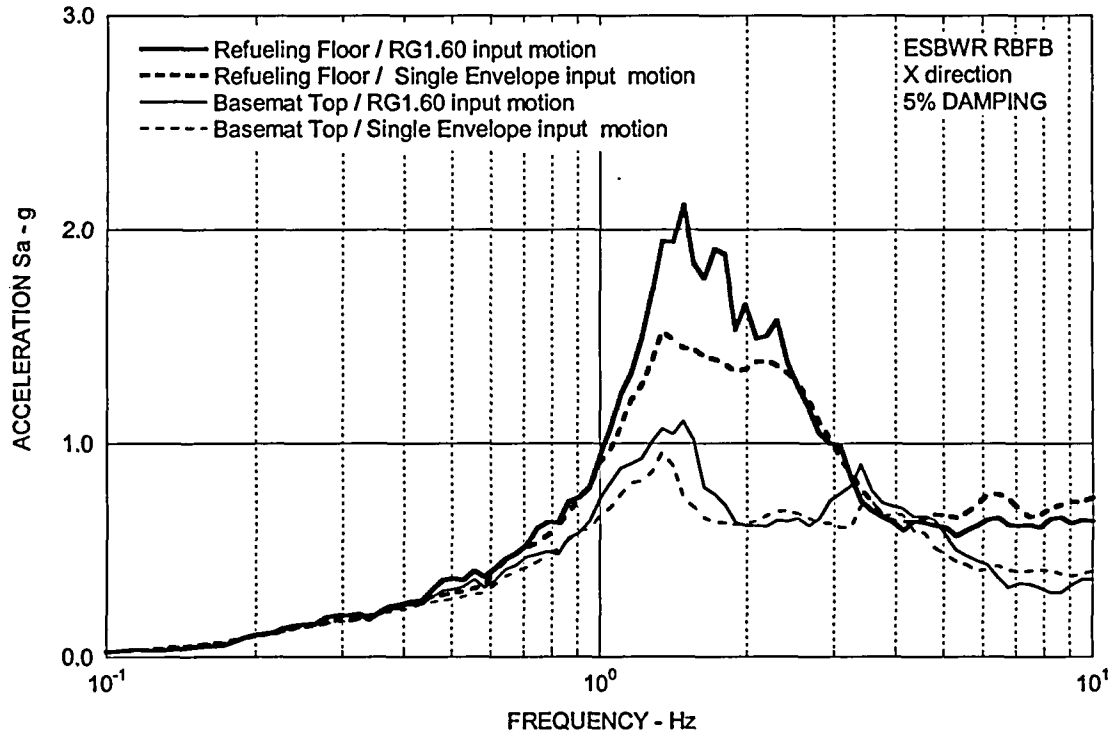

Figure 3.7-6 (11) FRS of RBFB (Soft site: X-Direction)

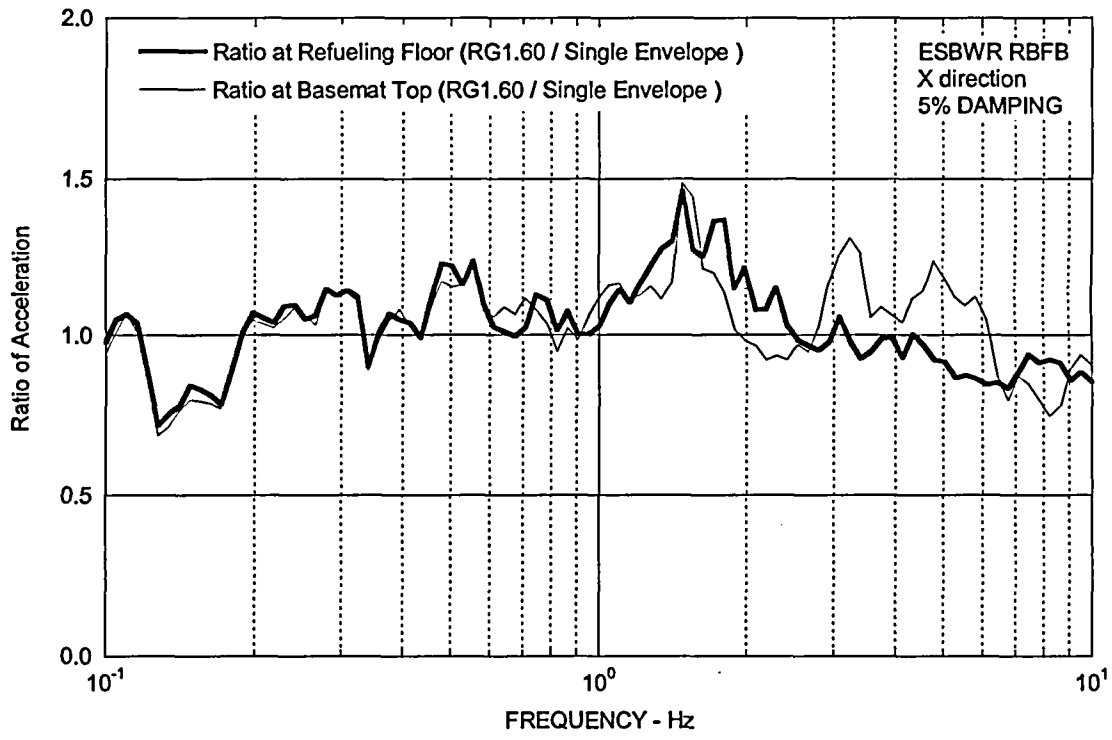

Figure 3.7-6 (12) Ratio of FRS (Soft site: X-Direction)

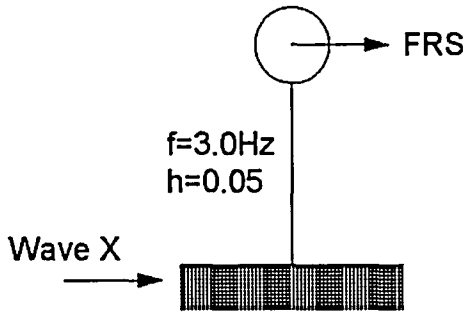

(a) Model for X-Direction

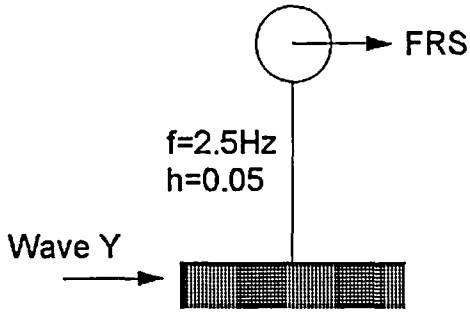

(b) Model for Y-Direction

Figure 3.7-6 (13) Single Degree of Freedom System

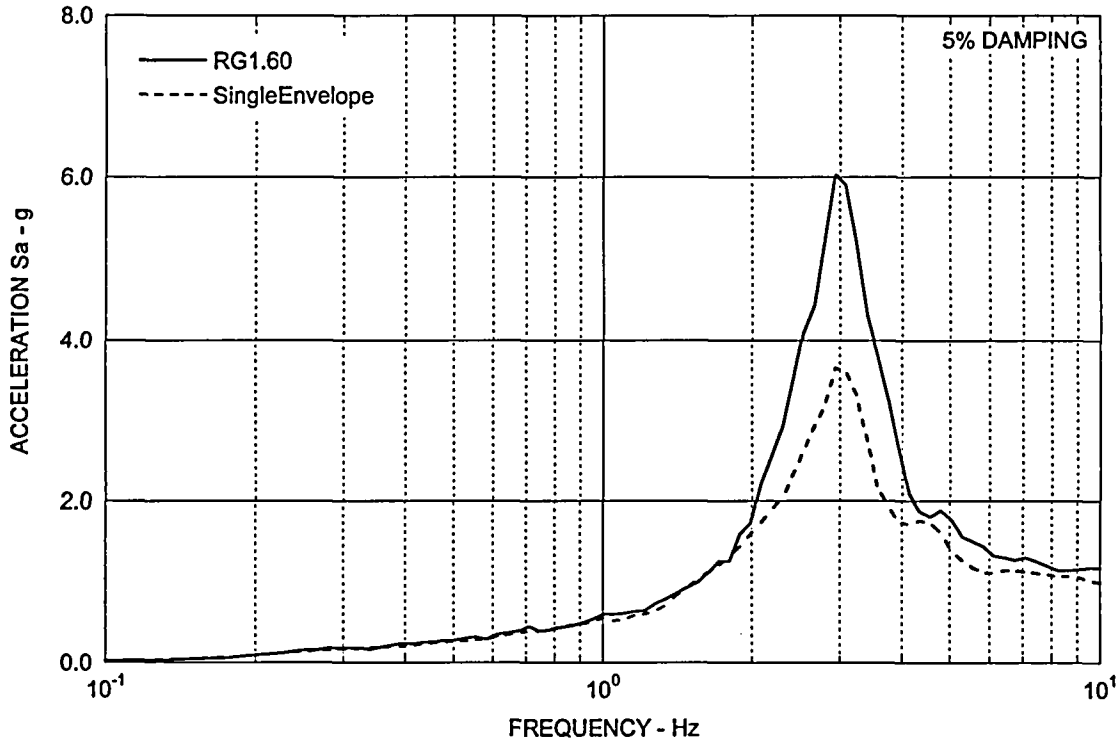

Figure 3.7-6 (14) FRS of Single Degree of Freedom System (X-Direction)

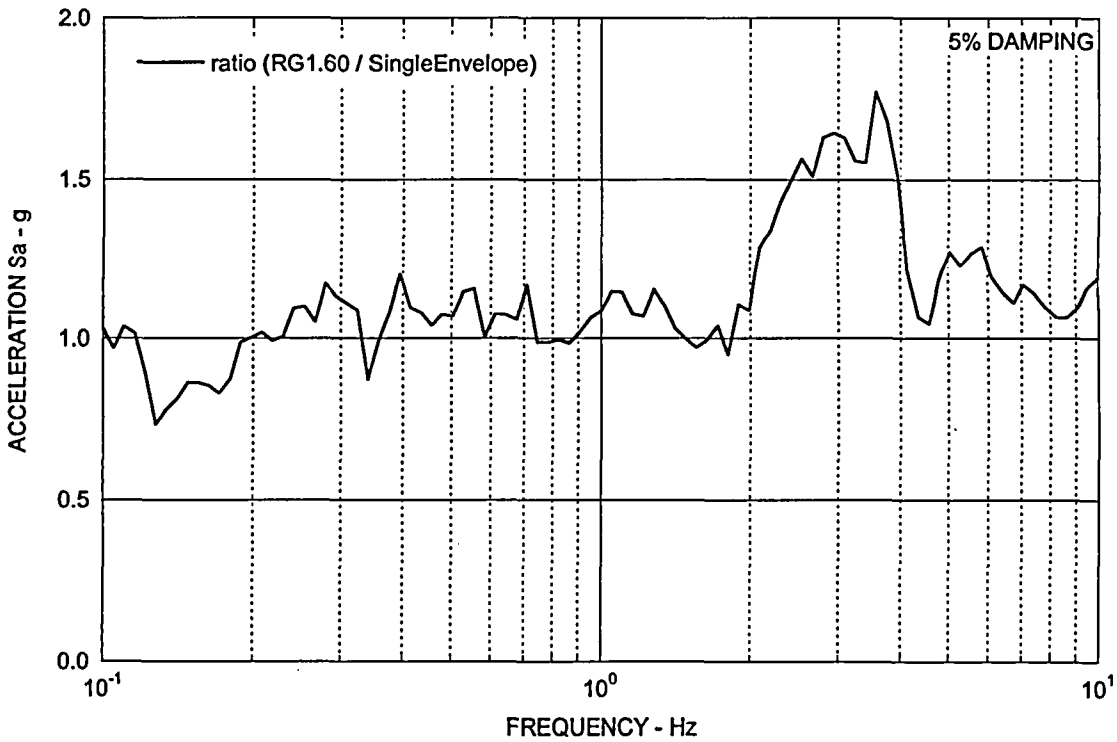

Figure 3.7-6 (15) Ratio of FRS (X-Direction)

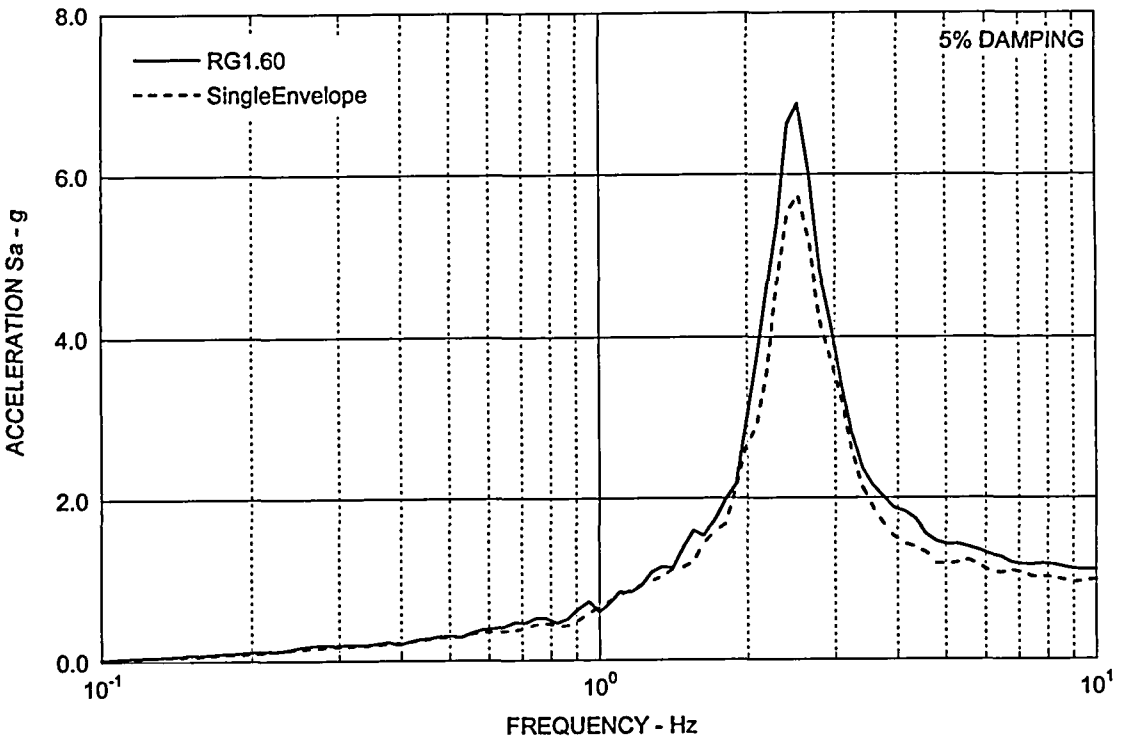

Figure 3.7-6 (16) FRS of Single Degree of Freedom System (Y-Direction)

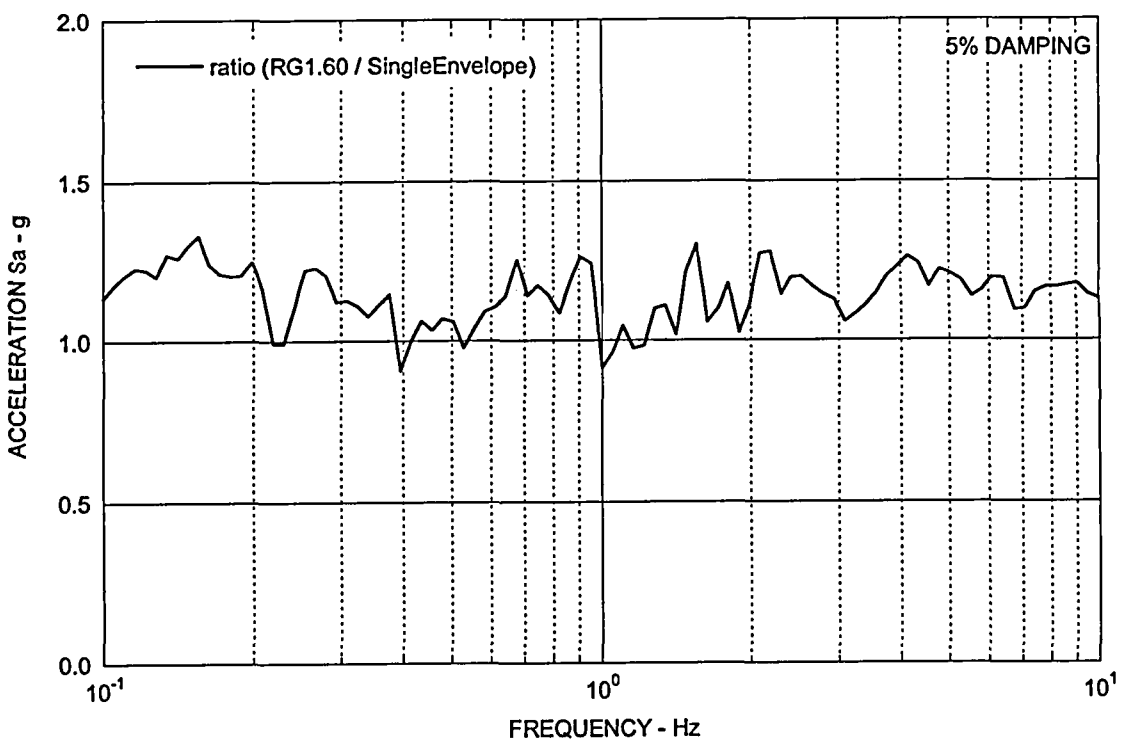

Figure 3.7-6 (17) Ratio of FRS (Y-Direction)

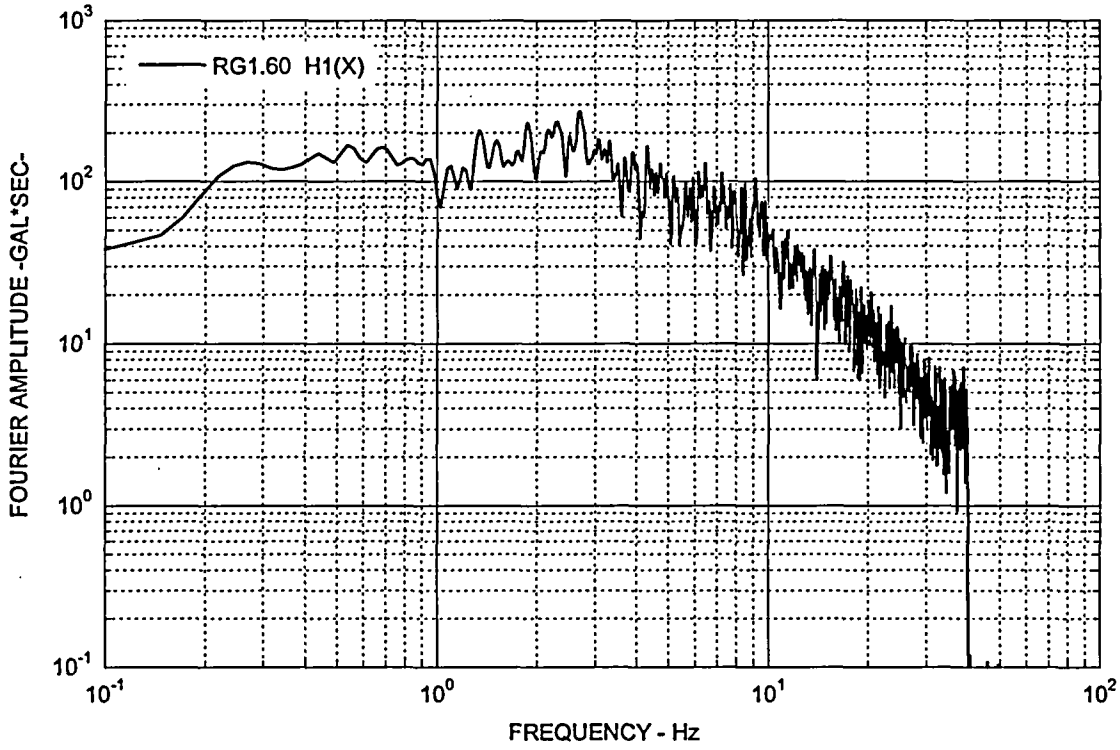

Figure 3.7-6 (18) Fourier Spectrum of RG 1.60 Input Motion (X-Direction)

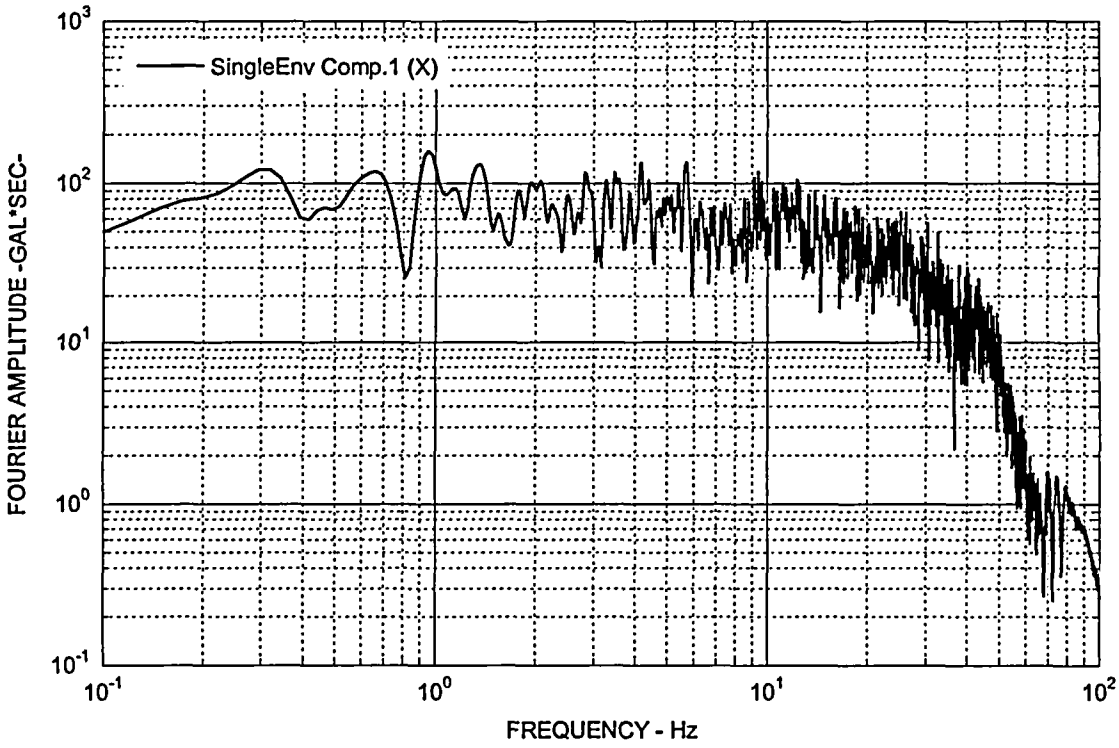

Figure 3.7-6 (19) Fourier Spectrum of Single Envelope Input Motion (X-Direction)

NRC RAI 3.7-48

DCD Section 3.7.2.14 describes the theory and analysis method for calculating the seismic Category I structure overturning moments. As a result of its review, the staff requests the applicant provide the following additional information:

In DCD Section 3.7.2.14, the applicant described the use of an energy method to evaluate the stability of structures against seismically induced overturning moments. The applicant is requested to provide a more detailed description of the analysis method, including an explanation of how the energy components for the embedment (W_p) and buoyancy (W_b) are determined, and the technical justification for the two equations given for the velocity terms (V_h and V_v).

GE Response

The analysis method to evaluate the stability of structures against seismically induced overturning moments is based on the energy method shown in the following reference.

> BC-TOP-4-A, Rev.3, *Seismic Analyses of Structures and Equipment for Nuclear Power Plants*, November 1974, Bechtel Power Corporation

Energy components for the embedment (W_p) is illustrated in Figure 3.7-48 (1).

Let d be the depth of embedment and d' be the submerged depth in case the ground water table is above the elevation of the base. The structure is assumed to rotate about the toe edge R (or L) for the overturning evaluation. To simplify the analysis for practical purposes, only the passive soil pressure developed on the toe-side is considered, and the wall frictions and the rather complicated actions of the soil on the other side of the structure are neglected. The passive pressure diagram conventionally constructed would be modified to be consistent with the assumption that the structure rotates about the edge R. Granular and free-draining soil conditions are also assumed. Figures 3.7-48 (1) (a) to (c) show the resultant idealized pressure diagram for different elevations of the ground water table when it is above the base (i.e., $d' > 0$). In these figures, the control parameter P_{dry} is given by:

$$P_{dry} = k_P \gamma_{soil} d \qquad (1)$$

and the parameter P_{sub} (for $d' > 0$) is given by:

$$P_{sub} = P_{dry} - d' \gamma_{water} \qquad (2)$$

where k_P, γ_{soil} and γ_{water} are the coefficients for passive soil pressure, the unit weight of soil and the unit weight of water, respectively.

For the structure to reach the overturning position, the additional work required to be done against the side soil is, according to Figure 3.7-48 (1) (a):

$$W_P = \int_0^d P(z)bz\tan\theta dz = b\tan\theta\int_0^d P(z)zdz \quad (3)$$

in which $p(z)$ is the idealized passive soil pressure at the elevation z above the base, θ is the angle of rotation at the overturning position, and b is the effective length of the structure normal to the plane of rotation. The effective length b is the structural dimension normal to the plane of rotation for rectangular structures, and 0.8 of the diameter for cylindrical structures. For the case that the ground water table is below the base, Eq. (3) gives:

$$W_{P(d'\le 0)} = \frac{1}{8}P_{dry}bd^2\tan\theta \quad (4)$$

and for the extreme case that the water table is at the ground surface:

$$W_{P(d'=d)} = \frac{1}{8}P_{sub}bd^2\tan\theta \quad (5)$$

Energy components for the buoyancy (W_b) is illustrated in Figure 3.7-48 (2).

When the ground water table is above the base ($d'>0$), the buoyant force has the effect of increasing the overturning potential of the structure. Such an effect would be appreciable when the submerged depth, d', is appreciable. It is accounted for in the analysis by subtracting from E_0 the work done by buoyant force.

The buoyant force acts at the centroid of the volume of the water displaced by the submerged portion of the structure, and its magnitude varies from position to position during the overturning process. At any position before overturning takes place, let the centroid of the displaced volume of water be located at a height of z above the elevation of the edge R and let the buoyant force be $B(z)$. Denoted by W_b, the work done by the buoyant force is equal to:

$$W_b = \int_{z_a}^{z_b} B(z)dz \quad (6)$$

in which, according to Figure 3.7-48 (2), z_a and z_b are the height of the centroid of buoyant force above the edge R for the equilibrium position (a) and the tipping over position (b) respectively. Note that is equal to $d'/2$. For practical purposes, Eq. (6) is approximated by:

$$W_b = (z_b + z_a)[B(z_b) - B(z_a)]/2 + B(z_a)(z_b - z_a) \quad (7)$$

The reason for the use of the two equations given for the velocity terms (V_h and V_v) is that the two expressions in DCD Tier 2 Equation 3.7-21 are the SRSS method of combination

to obtain the maximum value of total velocity response in view of non-simultaneous occurrence of the peak values of ground velocity and relative velocity response.

No DCD change was required in response to this RAI.

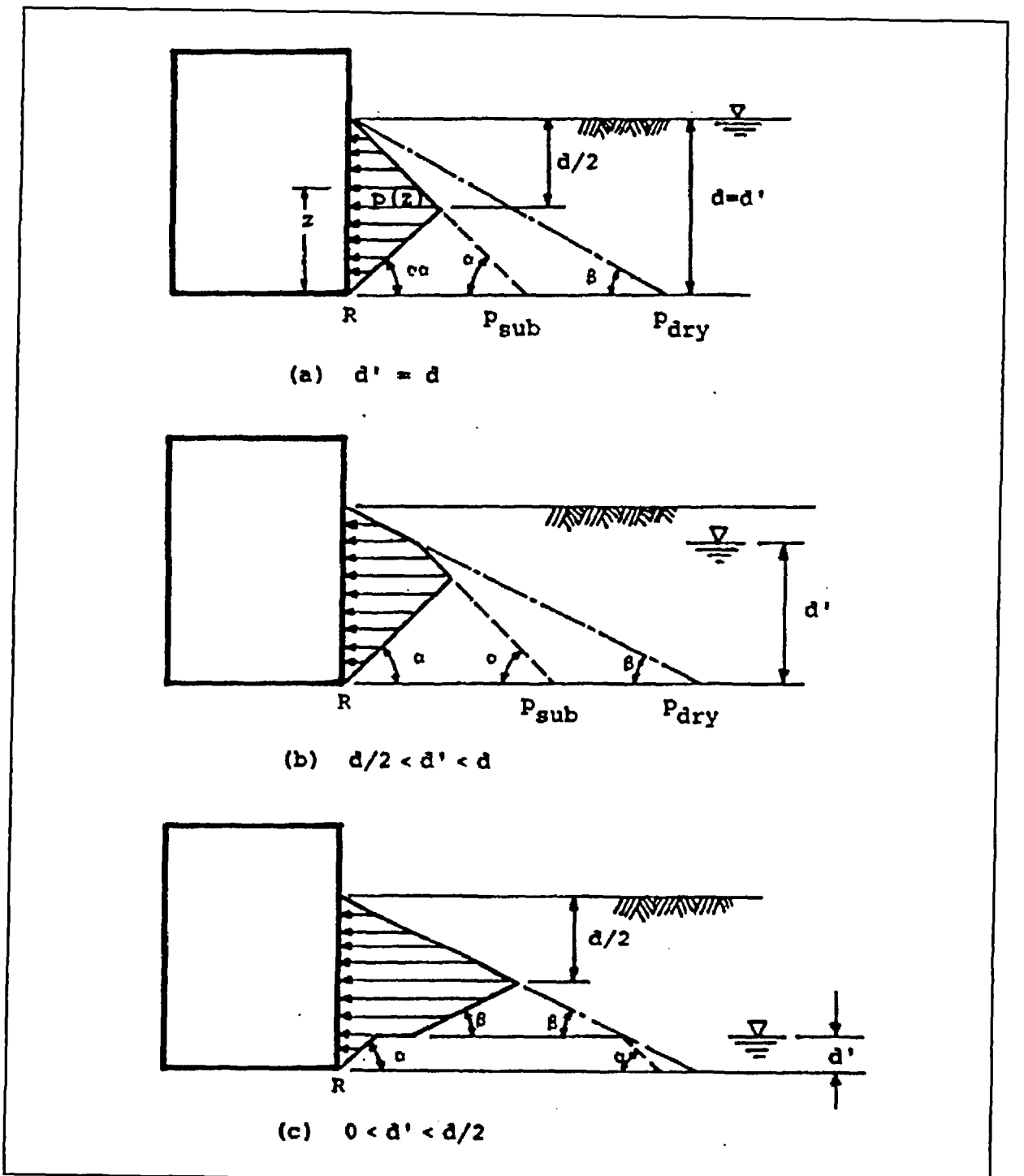

Figure 3.7-48 (1) Passive Soil pressure for Energy Components of Embedment

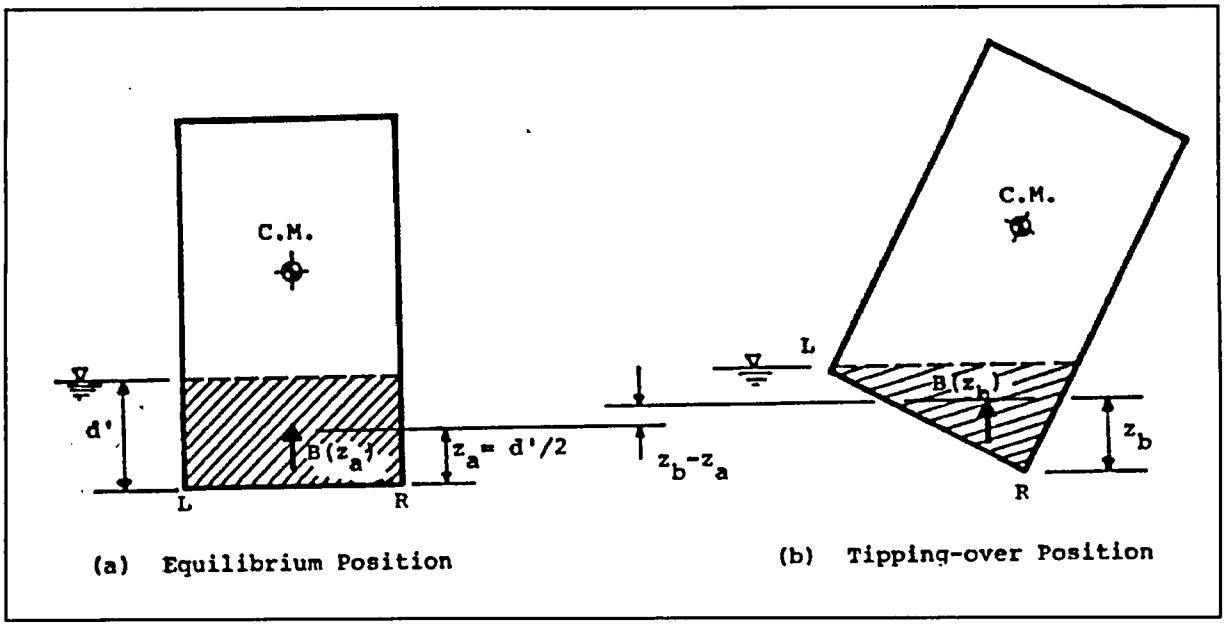

Figure 3.7-48 (2) Energy Components for Buoyancy

NRC RAI 3.7-48, Supplement 1

NRC Assessment Following the June 8, 2006 Audit

1. *Provide the corrected Equation 4-17 found in BC-TOP-4-A, Rev.3, Seismic Analyses of Structures and Equipment for Nuclear Power Plants, November 1974, Bechtel Power Corporation.*
2. *Provide the technical basis for using the SRSS method to combine the contribution from peak values of ground velocity and relative velocity.*

GE Response

1. GE found from its independent derivation that there is an error in Equation 4-17 in the above document. It should be corrected as follows:

   (Original Equation 4-17) $$W_b = (z_b + z_a)[B(z_b) - B(z_a)]/2 + B(z_a)(z_b - z_a)$$

   (Corrected Equation) $$W_b = (z_b - z_a)[B(z_b) - B(z_a)]/2 + B(z_a)(z_b - z_a)$$

2. The peak values of the horizontal ground velocity $(V_h)_g$ and the relative lateral velocity $(V_x)_i$ do not occur simultaneously. Similarly, the peak values of the vertical ground velocity $(V_v)_g$ and the relative vertical velocity $(V_z)_i$ do not occur simultaneously. Therefore, they are combined by the SRSS method as shown in DCD Tier 2 Equation 3.7-21.

No DCD change was required in response to this RAI supplement.

NRC RAI 3.7-48, Supplement 2

NRC Assessment Following the November 2, 2006 Audit

SRSS method of combining velocities in the original response is not acceptable. Provide an analysis using the Absolute Sum method of combining velocities. Revise also the tabulation of the safety factors in DCD Tier 2 Appendix 3G to reflect this change.

GE Response

GE will use the Absolute Sum method instead of the SRSS method for combining the velocity terms V_h and V_v.

DCD Tier 2 Subsection 3.7.2.14 will be revised in the next update as noted in the attached markup. DCD Tier 2 Table 3G.1-57 will also be revised to update the safety factors in the next revision.

position right above either edge of the base, the structure becomes unstable and may tip over. The mechanism of the rocking motion is like an inverted pendulum and its natural period is long compared with the linear, elastic structural response. Thus, with regard to overturning, the structure can be treated as a rigid body.

The maximum kinetic energy (E_s) can be conservatively estimated to be:

$$E_s = \frac{1}{2}\sum_i m_i[(V_h)_i^2 + (V_v)_i^2] \tag{3.7-20}$$

where $(V_h)_i$ and $(V_v)_i$ are the maximum values of the total lateral velocity and total vertical velocity, respectively, of mass m_i, and are computed as follows:

$$\begin{aligned} |(V_h)_i| &= |(V_x)_i| + |(V_h)_g| \\ |(V_v)_i| &= |(V_z)_i| + |(V_v)_g| \end{aligned} \tag{3.7-21}$$

where $(V_h)_g$ and $(V_v)_g$ are the peak horizontal and vertical ground velocity, respectively, and $(V_x)_i$ and $(V_z)_i$ are the maximum values of the relative lateral and vertical velocity of mass m_i.

Letting m_o be the total mass of the structure and base mat, the potential energy required to overturn the structure is equal to:

$$E_o = m_o g h + W_p - W_b \tag{3.7-22}$$

where h is the height to which the center of mass of the structure must be lifted to reach the overturning position, g is the gravity constant, and W_p and W_b are the energy components caused by the effects of embedment and buoyancy, respectively. Because the structure may not be a symmetrical one, the value of h is computed with respect to the edge that is nearer to the center of mass. The structure is defined stable against overturning when the ratio of E_o to E_s is no less than 1.1 for the SSE in combination with other appropriate loads.

3.7.3 Seismic Subsystem Analysis

This section applies to Seismic Category I (C-I) and Seismic Category II (C-II) subsystems (equipment and piping) that are qualified to satisfy the performance requirements according to their C-I or C-II designation. Input motions for the qualification are usually in the form of floor response spectra and displacements obtained from the primary system dynamic analysis. Input motions in terms of acceleration time histories are used when needed. Dynamic qualification can be performed by analysis, testing, or a combination of both, or by the use of experience data. This section addresses the aspects related to analysis only.

3.7.3.1 Seismic Analysis Methods

The methods of analysis described in Subsection 3.7.2.1 are equally applicable to equipment and piping systems. Among the various dynamic analysis methods, the response spectrum method is used most often. For multi-supported systems analyzed by the response spectrum method, the input motions can be either the envelope spectrum with Uniform Support Motion (USM) of all support points or the Independent Support Motion (ISM) at each support. Additional